AIP | The Journal of Chemical Physics

Branching ratios in the N+CH3 reaction: Formation of the methylene amidogen (H2CN) radical

G. Marston, F. L. Nesbitt, and L. J. Stief

Citation: The Journal of Chemical Physics **91**, 3483 (1989); doi: 10.1063/1.456878
View online: http://dx.doi.org/10.1063/1.456878
View Table of Contents: http://scitation.aip.org/content/aip/journal/jcp/91/6?ver=pdfcov
Published by the AIP Publishing

Branching ratios in the $N+CH_3$ reaction: Formation of the methylene amidogen (H_2CN) radical

G. Marston,[a] F. L. Nesbitt,[b] and L. J. Stief
Code 691, Astrochemistry Branch Laboratory for Extraterrestrial Physics, NASA/Goddard Space Flight Center, Greenbelt, Maryland 20771

(Received 11 April 1989; accepted 30 May 1989)

The branching ratios for the reaction $N + CH_3 \rightarrow$ Products, have been determined in a discharge-flow system coupled with mass-spectrometric detection of both reactants and products. The major products are $H_2CN + H$, with about 10% of the reaction proceeding to give $HCN + H_2$. Experiments carried out on the reaction of N atoms with the deuterated methyl radical showed that the branching ratio for formation of $D_2CN + D$ is about 0.9 and for $DCN + D_2$ formation about 0.1 independent of T from 200 to 363 K. The results are consistent with the energetics and orbital symmetry properties of the reactant and product molecules. Implications for the atmosphere of Titan are discussed.

INTRODUCTION

The reaction of N atoms with methyl radicals is believed to be a major source of HCN in the upper atmosphere of Titan,[1] and has recently been suggested as one of the processes which lead to HCN formation in O-rich circumstellar clouds.[2] The reaction is also thought to play an important role in the generation of NO_x species in combustion processes,[3] and in the reaction between active nitrogen and hydrocarbons.[4]

The kinetics of the reaction have recently been studied in this laboratory; the reaction is fast [k_1 (298 K) $= 8.5\times10^{-11}$ cm^3 s^{-1} [5]] and has a temperature dependence which may be non-Arrhenius.[6] In order to fully understand the processes mentioned above it is necessary not only to know the kinetics of the overall reaction but also the relative importance of the various product channels. There are three thermodynamically accessible channels

$$N + CH_3 \rightarrow HCN + H_2, \quad \Delta H = -490 \text{ kJ mol}^{-1}, \tag{1a}$$

$$N + CH_3 \rightarrow HCN + 2H, \quad \Delta H = -54 \text{ kJ mol}^{-1}, \tag{1b}$$

$$N + CH_3 \rightarrow H_2CN + H, \quad \Delta H = -153 \text{ kJ mol}^{-1}. \tag{1c}$$

Although other channels exist (e.g., abstraction to give $NH + CH_2$) they are endothermic. There have been no direct studies to determine the products of reaction (1). The most frequently assumed products are $HCN + 2H$.[1-3] However, Safrany[4] has suggested that channel (1c) is the most important branch of the reaction. His proposal was based on analogy with the $O + CH_3$ reaction and the results of active nitrogen/hydrocarbon experiments. The object of the present work was to determine directly the branching ratios for channels (1a), (1b) and (1c).

[a] NAS/NRC Postdoctoral Research Associate.
[b] Research Associate, Chemistry Department, Catholic University of America, Washington, D.C. 20017

EXPERIMENTAL

The apparatus used in this work was a discharge-flow mass spectrometer system and has been described in detail elsewhere.[7,8] The flow tube was built from 3 cm diameter uncoated Pyrex and was ca. 60 cm long. Reagents were added through one of three inlets at the back of the flow tube or through a movable injector. The detection system consisted of a collision-free sampling arrangement coupled to a quadrupole mass spectrometer which was operated at low electron energies ($<$ 20 eV) to minimize fragmentation. Reaction vessel temperatures were controlled by circulating heating or cooling fluids through a jacket surrounding the flow tube. Experiments were carried out at approximately 1 Torr total pressure with a linear flow velocity between 1500–3200 cm s^{-1}, depending on temperature. Gas flows were measured and controlled by electronic flow meters (ASM International, N.V.)

Nitrogen atoms were generated by passing N_2 (1%–10% in He) through a microwave discharge (70 W, 2450 MHz). Absolute concentrations were determined using the $N + NO$ titration reaction as has been described elsewhere.[6]

Methyl radicals were generated and calibrated using the titration reactions[5]

$$F + CH_4 \rightarrow HF + CH_3. \tag{2}$$

F atoms were produced by passing CF_4 ($\sim$0.1% in He) through a microwave discharge (70 W, 2450 MHz). For some experiments the deuterated methyl radical was used. CD_3 was generated using the $F + CD_4$ reaction and absolute concentrations were estimated in the same way as for CH_3.

Deuterium atoms were formed by passing D_2 through a microwave discharge (70 W, 2450 MHz). A number of methods were used to calibrate the detection system for D atoms. In the first method the change in signal from D_2 at $m/e = 4$ (electron energy = 18 eV) was used to calculate the loss in D_2 on turning on the microwave discharge. The D-atom concentration is equal to twice the loss in D_2. Signal at $m/e = 2$ (electron energy = 18 eV) was then plotted as a

function of the D-atom concentration. Using this method the signal at $m/e = 2$ is directly related to the concentration of D atoms at the sampling pinhole.

The second method was identical to the first, but NO_2 was added through the sliding injector. D atoms were destroyed in the reaction

$$D + NO_2 \rightarrow OD + NO \quad (3)$$

and consequently could not recombine on the flow tube walls. By comparison with the reaction of H atoms with NO_2,[9] reaction (3) is expected to be very fast. In this case the D-atom signal was related to the D-atom concentration at the position of the sliding injector. In the absence of wall losses, both methods would give the same result. In fact there was a significant loss of D atoms on the wall. By varying the injector position a rate constant for the destruction of D atoms on the flow tube walls of about 20 s^{-1} was deduced.

In order to ensure accurate determinations of D-atom concentrations, a third method was used to provide a check on the other two. The gas flows were the same as for the second method but the D-atom concentration was determined by measuring the change in NO_2 signal at $m/e = 46$ (electron energy = 18 eV) when the discharge was turned on. Under the low D-atom concentrations prevalent in our system the change in $[NO_2]$ is equal to the D-atom concentration.[10] In principle, the second and third methods should give identical results, as was found to be the case and is illustrated in Fig. 1. The minimum detectable level of D atoms was 5×10^{10} cm^{-3} at a signal-to-noise ratio of 1 and a 40 s integration time.

Calibrations for the molecular species HCN, H_2, and D_2 were obtained by monitoring the signal at the appropriate mass as known flows of the reagents were admitted to the flow tube.

During most of the experiments, N and F atoms were added at the back of the flow tube, while CH_4 (or CD_4) was introduced through the movable injector. Details of experiments carried out under different conditions will be given at the appropriate place in the text.

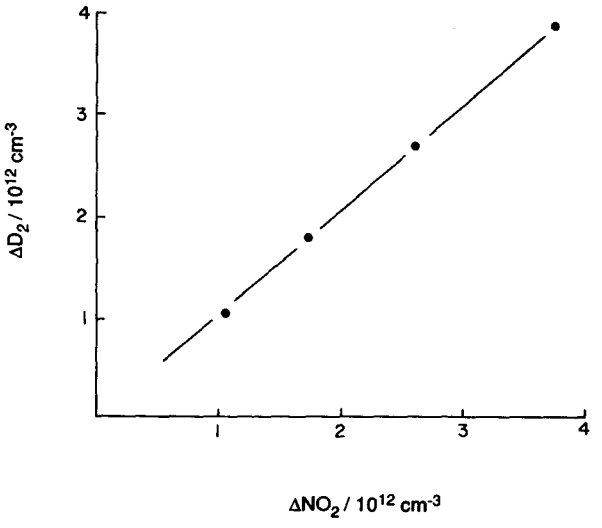

FIG. 1. Plot showing correlation between D-atom measurements obtained from measuring ΔD_2 (in presence of NO_2) and ΔNO_2.

Nitrogen dioxide was obtained from Matheson at a stated purity of 99.5%. The gas was mixed with excess oxygen and stored overnight prior to use in order to convert impurity NO to NO_2. The NO_2 was then trapped in a cold finger, the oxygen was pumped off and the pure NO_2 was diluted in helium ready for use. CD_4 (isotopic purity = 99%, MSD isotopes), D_2 (isotopic purity = 99.5%, MSD isotopes), and H_2 (stated purity = 99.999%, Matheson) were used after dilution in helium without further purification. HCN (Matheson) was obtained as an 8.1% mixture in helium. It was used directly or after further dilution in helium. Sources for He, N_2, NO, CH_4, and CF_4 are given in Ref. 5 along with reagent purities and methods used for further purification.

RESULTS

Before presenting the specific results obtained in this study, a short discussion will be given describing the particular difficulties encountered in measuring branching ratios for the $N + CH_3$ reaction.

When measuring the branching ratio of a reaction, the most direct method is to measure the concentration of product formed for a given loss of reactant. The ratio of these two quantities then gives the fraction of reaction leading to that particular product. Unfortunately, such a direct approach is not always feasible as is illustrated by the title reaction

$$N + CH_3 \rightarrow HCN + H_2, \quad (1a)$$

$$N + CH_3 \rightarrow HCN + 2H, \quad (1b)$$

$$N + CH_3 \rightarrow H_2CN + H. \quad (1c)$$

Measuring changes in reactant concentration is relatively straightforward, but the products are either reactive or can be generated by secondary processes (or both). HCN is not formed directly in channel (1c) but likely fates for the H_2CN radical are

$$N + H_2CN \rightarrow NH + HCN \quad (4)$$

or

$$H_2CN + \text{wall} \rightarrow HCN + H_w, \quad (5)$$

where H_w indicates that the H atom is bound to the wall of the flow tube. As a result HCN yields give little information about the branching ratios.

Similarly, H atoms generated in channels (1b) and (1c) can recombine on the reaction vessel walls to give H_2, thus frustrating efforts to measure the fraction of reaction forming this molecular species. H atoms provide difficulties because they are reactive, being destroyed on the flow tube walls, and they are generated by reaction between NH [a product of reaction (4)] and N atoms

$$N + NH \rightarrow N_2 + H. \quad (6)$$

Furthermore, mass-spectrometric sensitivity at $m/e = 1$ is poor and consequently, H atoms are difficult to detect.

Finally, the radical H_2CN is reactive[11] and there are no known calibration procedures available for the species.

Because of these difficulties it was often necessary to use less direct methods to determine the branching ratios. Information from rates of formation of products, numerical simu-

lations, and isotopic substitution were all used to determine the relative importance of the channels of reaction (1).

Study at 298 K

Although absolute yields of HCN can tell us little about the branching ratios of reaction (1), the rate of formation of the molecule can provide information. Rate constants obtained from the formation of products actually reveal information about the decay of reactants. Signal due to HCN at $m/e = 27$ was monitored as a function of contact time and the expression

$$\ln\left\{\frac{[\mathrm{HCN}]_\infty - [\mathrm{HCN}]}{[\mathrm{HCN}]_\infty}\right\} = k'_f t \qquad (7)$$

was used to obtain pseudo-first-order rate constants for the formation of HCN. In Eq. (7), [HCN] is the HCN concentration at time t, $[\mathrm{HCN}]_\infty$ is the HCN concentration at $t = \infty$ and k'_f is the pseudo-first-order rate constant for formation of HCN. These rate constants were found to be dependent on the N-atom concentration, and a plot of k'_f vs. $[\mathrm{N}]_0$ is displayed in Fig. 2. The slope of the line is $(5.2 \pm 1.8) \times 10^{-11}\ \mathrm{cm^3\ s^{-1}}$ and it is concluded that there is a species which is destroyed by N with a rate constant of $5.2 \times 10^{-11}\ \mathrm{cm^3\ s^{-1}}$, and which generates HCN as one of its primary products.

The N + CH_3 reaction has a rate constant[5,6] of $8.5 \times 10^{-11}\ \mathrm{cm^3\ s^{-1}}$, a value significantly higher than that obtained from Fig. 2. The implication is that HCN is not being formed directly via reaction (1). Another possibility is that H_2CN is being generated in reaction (1c) and that this radical then reacts with N atoms to give HCN. Using low electron energies ($\sim$12 eV) to avoid interference from ground state and vibrationally excited[6] N_2, signal was detected at $m/e = 28$ in the presence of both N and CH_3. When CH_3 was replaced by CD_3, product signal was observed at $m/e = 30$; for these experiments higher electron energies (18 eV) could be used as there were no interference problems at this mass. Furthermore, the signals at $m/e = 28$ and $m/e = 30$ exhibited similar temporal behavior: initially they increased with time before reaching a maximum and then falling off. These profiles are consistent with a reactive species being formed by the N + CH_3 or N + CD_3 reactions followed by its subsequent destruction.

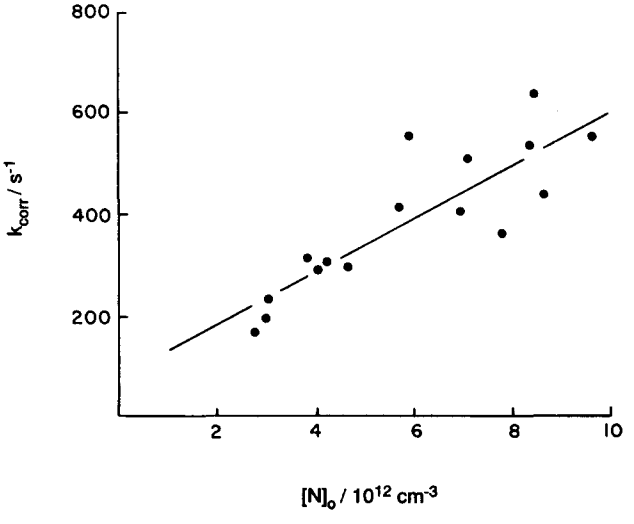

FIG. 2. Plot of k_{corr} vs. $[\mathrm{N}]_0$ obtained from HCN formation rates. k_{corr} is the pseudo-first-order rate constant corrected for axial diffusion as described in Refs. 5 and 6.

It is concluded that the signals at $m/e = 28$ and $m/e = 30$ are due to H_2CN, and D_2CN, respectively. Using the parts of the time profiles where the radical decreased with time, pseudo-first-order rate constants for the decay of the species were measured as a function of $[\mathrm{N}]_0$. These data will be presented elsewhere.[11] For the time being we should note that the apparent bimolecular rate constant obtained in this way is $(4.9 \pm 1.1) \times 10^{-11}\ \mathrm{cm^3\ s^{-1}}$. Within experimental error this value is identical to that obtained from the formation of HCN, and the obvious conclusion is that most, if not all, of the HCN is generated in the reaction

$$\mathrm{N + H_2CN \rightarrow NH + HCN.} \qquad (4)$$

Measurements of the HCN yield were also carried out. Under conditions of excess N and long contact times [HCN] was monitored as a function of $[\mathrm{CH_3}]_0$. A plot of [HCN] vs $[\mathrm{CH_3}]_0$ yielded a slope of 0.90 ± 0.15 (95% confidence). It appears therefore that the dominant channel in the reaction of N atoms with H_2CN is that leading to NH + HCN as products.

Further evidence was obtained by watching the change in N-atom concentration on reaction with CH_3. These experiments were performed by monitoring the N-atom signal at $m/e = 14$ (electron energy = 16 eV) and comparing the change with the initial CH_3 concentration. The experiments revealed that under conditions of excess N and long contact times, about 2.5 N atoms were destroyed for every CH_3 radical. The following mechanism is consistent with these results

$$\mathrm{N + CH_3 \rightarrow H_2CN + H,} \qquad (1c)$$

$$\mathrm{N + H_2CN \rightarrow NH + HCN,} \qquad (4)$$

$$\mathrm{N + NH \rightarrow N_2 + H.} \qquad (6)$$

That the efficiency for destruction of N atoms is 2.5 rather than 3 may be due to heterogeneous losses of reactive species, or, as will be discussed later, the fact that channels (1a) or (1b) make a small contribution to the total rate.

The experiments described in the previous paragraphs give strong support to the idea that the major channel for reaction (1) is that leading to H_2CN + H. However, the possibility that the two remaining channels play a minor role cannot be excluded. Experiments were carried out to try and assess the importance of channels (1a) and (1b).

Information from the yield of H_2 formation is confused by the molecule being formed in the heterogeneous recombination of H atoms. However, the reaction

$$\mathrm{H + Cl_2 \rightarrow HCl + Cl} \qquad (8a)$$

is very rapid[12] (k_8 (298 K) $= 2.2 \times 10^{-11}\ \mathrm{cm^3\ s^{-1}}$) and Cl_2 can be used to "scavenge" H atoms. For these experiments N atoms and CH_3 radicals were admitted at the back of the flow tube by adding CH_4, discharged N_2 and discharged CF_4 through the fixed side arms. The concentration of N atoms was $\sim 1.5 \times 10^{13}\ \mathrm{cm^{-3}}$, thus ensuring complete con-

version of CH_3 to products in a short time. A few centimeters downstream molecular chlorine ($[Cl_2] = 2\times10^{13}$ cm^{-3}) was added through the sliding injector. The position of the injector was such that the N + CH_3 reaction was effectively complete on addition of Cl_2, thus avoiding complications from secondary reactions of Cl_2. However, the injector was sufficiently close to the reaction zone that only a small fraction of H atoms could recombine on the walls. $[H_2]$ was monitored as a function of $[CH_3]_0$, the experiments also being repeated for the deuterated radical. The results are plotted in Fig. 3; the slopes of the lines are both about 0.1, no isotope effect being observed. The simplest explanation of the results is that the channel

$$N + CH_3 \rightarrow HCN + H_2 \quad (1a)$$

accounts for 10% of the total reaction, although the possibility that H_2 is generated by heterogeneous reaction of H_2CN can not be excluded.

Determining the extent to which channel (1b) occurs is difficult as ultimately both (1b) and (1c) generate two H atoms for every CH_3 radical destroyed, either directly

$$N + CH_3 \rightarrow HCN + 2H \quad (1b)$$

or indirectly via the sequence of reactions

$$N + CH_3 \rightarrow H_2CN + H, \quad (1c)$$

$$N + H_2CN \rightarrow NH + HCN, \quad (4)$$

$$N + NH \rightarrow N_2 + H, \quad (6)$$

overall

$$3N + CH_3 \rightarrow N_2 + HCN + 2H. \quad (8b)$$

The difficulties can be partially overcome if secondary reactions are suppressed by using only small concentrations of N atoms. Discrimination between the two channels can then be achieved but the results must be interpreted using numerical simulations. At first sight HCN would appear to be the easiest product to monitor as it is stable and so does not undergo further reaction. However, destruction of H_2CN on the walls seems likely to generate HCN and frustrate the interpretation of the results. The mass-spectrometer sensitivity at $m/e = 1$ is poor and so the formation of D atoms from the reaction N + CD_3 was investigated.

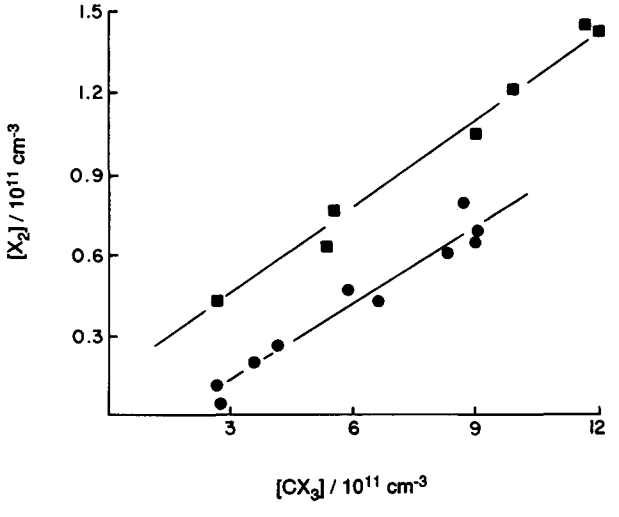

FIG. 3. Plot to determine yield of X_2 from the N + CX_3 reaction, where $X = H(\blacksquare)$ and $X = D(\bullet)$.

TABLE I. Reactions used to model formation of D and D_2CN. Second order rate constants in units of cm^3 s^{-1}, first-order rate constants in units of s^{-1}. Values given to 2 significant figures.

Reaction	$k(200)$	$k(298)$	$k(363)$	Ref.
F + CD_4 → DF + CD_3	2.0×10^{-11}	5.0×10^{-11}	6.9×10^{-11}	13,14
N + CD_3 → DCN + D_2	6.4×10^{-12}	8.5×10^{-12}	1.4×10^{-11}	This work
N + CD_3 → DCN + 2D	0	4.3×10^{-12}	0	Fitted
N + CD_3 → D_2CN + D	5.8×10^{-11}	7.2×10^{-11}	1.3×10^{-10}	Fitted
N + D_2CN → ND + DCN	3.9×10^{-11}	4.4×10^{-11}	6.6×10^{-11}	11
CD_3 + CD_3 → C_2D_6	5.0×10^{-11}	5.0×10^{-11}	5.0×10^{-11}	15[a,b]
D + CD_3 → CD_4	2.6×10^{-11}	2.6×10^{-11}	2.6×10^{-11}	15[a,b]
N + ND → N_2 + D	1.6×10^{-1}	1.9×10^{-10}	2.1×10^{-10}	15[a]
D_2CN → wall	180	240	120	11
D → wall	20	20	100	This work

[a]Rate constants assumed equal to those for the undeuterated species.
[b]When the T dependence was unknown, rate constants at 298 K were used at all temperatures.

Signal at $m/e = 2$ was monitored as a function of $[N]_0$ ($[N]_0 \leqslant [CD_3]_0$) for a fixed contact time and CD_3 concentration. The model listed in Table I and rate constant values taken from the literature[11,13-15] were then used to obtain the value of k_{1bD} which gave the best agreement with experiment. The goodness of fit was assessed by the magnitude of $S(D)$

$$S(D) = \sum_i \left\{ \frac{[D]_{e,i} - [D]_{c,i}}{[D]_{e,i}} \right\}^2 \quad (9)$$

where $[D]_{e,i}$ are the experimental D-atom concentrations and $[D]_{c,i}$ are the calculated values. The best fit was obtained with 5% of the reaction going to DCN + 2D [α_{1bD}(298 K) = 0.05] and 85% of the reaction giving D_2CN + D [α_{1cD}(298 K) = 0.85]. An estimate of the errors can be obtained from the expression[16]

$$\sigma_\alpha^2 = \sum_i \sigma_i^2 (\partial\alpha/\partial [D]_{e,i})^2, \quad (10)$$

where σ_α is the error in the branching ratio α, σ_i are the errors in the D-atom concentrations, $[D]_{e,i}$ and $(\partial\alpha/\partial[D]_{e,i})$ are the sensitivity coefficients describing the dependence of α on changes in the D-atom concentrations, $[D]_{e,i}$. The errors, σ_i, can be estimated in the usual way. The sensitivity coefficients were obtained by changing the D-atom concentrations in the model one by one and observing the changes in α. The error in α_{1cD} (298 K) obtained in this way is about 30%, the uncertainty including statistical errors at the 95% confidence level and a 10% systematic error resulting from the D-atom calibration. Figure 4 shows the experimental plot of [D] vs $[N]_0$ compared with the best-fit curve.

From the evidence just described, the following branching ratios are obtained or reaction (1D):

$$N + CD_3 \rightarrow DCN + D_2, \quad \alpha_{1aD}(298\ K) = 0.10 \pm 0.02, \quad (1aD)$$

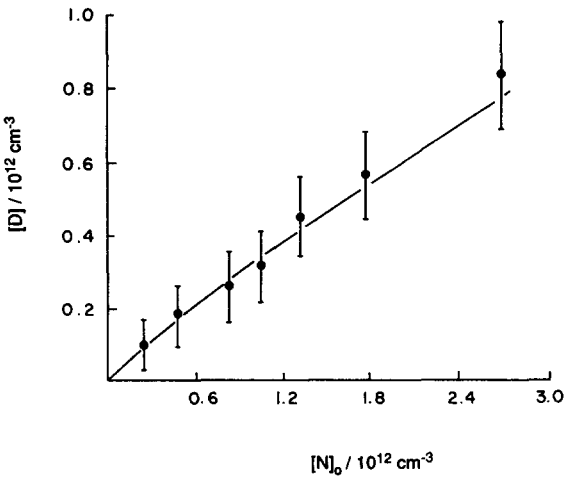

FIG. 4. Plot of [D] vs $[N]_0$. Experimental points (●). Computer fit (—), α_{1bD} (298 K) = 0.05. $[CD_3]_0 = 1.7\times10^{12}$ cm^{-3}.

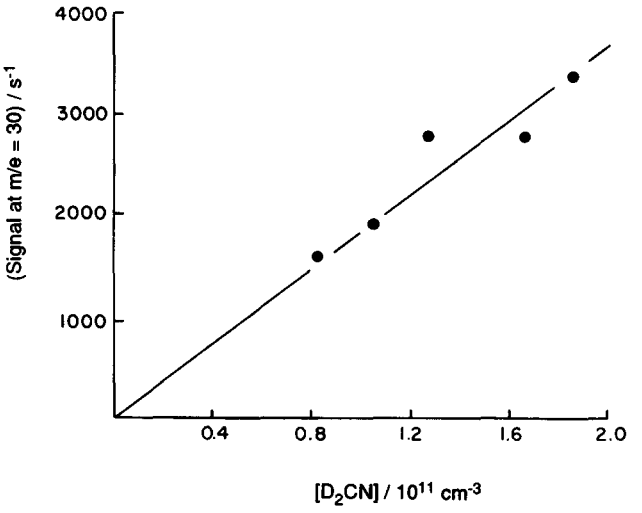

FIG. 5. Calibration for D_2CN at 298 K.

$$N + CD_3 \rightarrow DCN + 2D, \quad \alpha_{1bD}(298\text{ K}) = 0.05^{+0.25}_{-0.05}, \tag{1bD}$$

$$N + CD_3 \rightarrow D_2CN + D, \quad \alpha_{1cD}(298\text{ K}) = 0.85^{+0.07}_{-0.25}. \tag{1cD}$$

Our experiments show that the fraction of reaction (1) leading to HCN + H_2 is about 10% and the fraction leading to H_2CN + H is large. These conclusions are consistent with those determined for reaction (1D), there apparently being no isotope effect. Therefore, it is assumed that the branching ratios for reaction (1) are the same as those quoted above for reaction (1D). The results at 298 K are summarized in Table II.

Having thus determined the branching ratios at room temperature it was possible to calibrate for the D_2CN radical. D_2CN was generated with known initial concentrations of CD_4 and the atomic species F and N. The signal at $m/e = 30$ was recorded at its maximum value and the concentration of D_2CN was then calculated using the model listed in Table I. Figure 5 displays a plot of signal at $m/e = 30$ vs $[D_2CN]$. The minimum detectable level of D_2CN is estimated to be 5×10^9 cm^{-3} at a signal-to-noise ratio of 1 and 10 s integration time. From this calibration curve signals from D_2CN at other temperatures can be converted to concentrations and then compared with model calculations. Although in principle this calibration could also be carried out for signal at $m/e = 28$ from H_2CN, in practice it was not feasible. Because of interference from excited N_2 it was necessary to work at low electron energies, considerably reducing the amount of signal observed, and consequently the precision of the measurements. Therefore, calibrations were not performed for H_2CN.

TABLE II. Branching ratios for reactions (1) and (1D) at 298 K.

Channel	α(298 K)	Method
(1a) HCN + H_2	0.10 ± 0.02	$[H_2]$ vs $[CH_3]$ in presence of Cl_2.
(1aD) DCN + D_2	0.10 ± 0.02	$[D_2]$ vs $[CD_3]$ in presence of Cl_2.
(1b) HCN + 2H	~0	Rate of formation of HCN/Rate of decay of H_2CN
(1bD) DCN + 2D	$0.05^{+0.25}_{-0.05}$	Computer simulation of D-atom formation
(1c) H_2CN + H	~1	Rate of formation of HCN/Rate of decay of H_2CN
(1cD) D_2CN + D	$0.85^{+0.07}_{-0.25}$	Computer simulation of D-atom formation

Study at 200 K

Experiments were carried out to determine the yield of D_2 formed in the reaction N + CD_3. Just as for the room temperature study the measurements were done in the presence of Cl_2, to avoid interference caused by D-atom recombination. The result obtained was that approximately 10% of the reaction proceeded to give DCN + D_2, just as observed at 298 K.

Having determined the branching ratios for reaction (1) at room temperature and obtained a calibration for D_2CN, it was possible to determine the branching ratios (at least for the deuterated reaction) at 200 K, more or less directly. Using the calibration curve displayed in Fig. 5, D_2CN concentrations were calculated from observed signals at $m/e = 30$ when N atoms and CD_3 were present together in the flow tube. The change in sensitivity of the detection system on lowering the temperature to 200 K was accounted for by observing the signal obtained from a known concentration of NO added to the flow tube. Concentrations of D_2CN were then calculated using numerical integration for various values of the branching ratios, given the known initial conditions. The value for the branching ratios which gave the best fit with the data was determined by minimizing $S(D_2CN)$ in the expression

$$S(D_2CN) = \sum_i \left\{ \frac{[D_2CN]_{e,i} - [D_2CN]_{c,i}}{[D_2CN]_{e,i}} \right\}^2, \tag{11}$$

where $[D_2CN]_{e,i}$ are the D_2CN concentrations estimated from the calibration and $[D_2CN]_{c,i}$ are those predicted by the simulation. The best fit was obtained with about 90% of

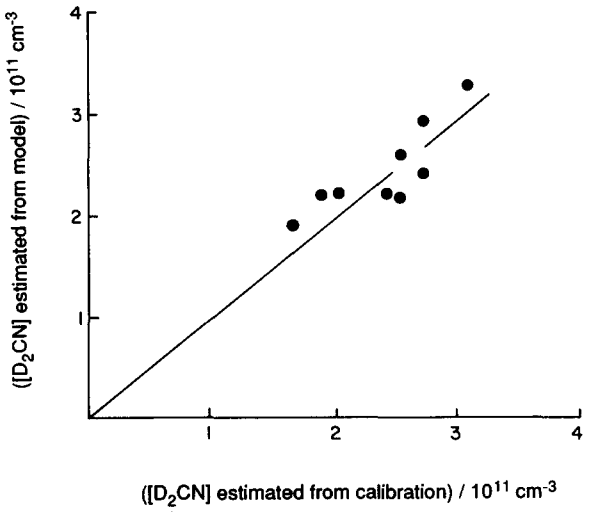

FIG. 6. Determination of branching ratio at 200 K. Plot of ([D_2CN] from model) vs ([D_2CN] from calibration).

the reaction going to $D_2CN + D$ and none going to $DCN + 2D$. Figure 6 shows a plot of $[D_2CN]_e$ vs. $[D_2CN]_c$, using the best fit parameters. The correlation between the two quantities is reasonable ($r = 0.71$), and the slope of the line is unity within experimental error. The experimental errors arising from this analysis are expected to be fairly large and our estimates for the branching ratios of reaction (1D) are listed in Table III. By analogy with the results at room temperature it is proposed that these branching ratios are the same for the reaction of N atoms with the undeuterated methyl radical. Support for this conclusion comes from the fact that H_2CN is relatively easily detected at 200 K.

In principle, the experiments performed at room temperature on the rate of formation of HCN could be repeated at this temperature. However, the difference between k_1 (200 K)[6] and k_4 (200 K)[11] is smaller than at room temperature, while the statistical errors associated with these measurements are actually larger. Given the difficulty of measuring rate constants by the formation of products, it seems likely that measurements of the rate of formation of HCN would be unable to distinguish between the two possible sources of the molecule. Consequently, these experiments were not carried out.

Attempts were made to repeat the room temperature experiments on D-atom formation at this lower temperature. However, the results were somewhat inconsistent and suggested that virtually none of reaction (1D) yielded D_2CN. These observations are completely at odds with the fact that D_2CN was easily detected. One possible explanation is that destruction of D_2CN on the walls of the flow tube resulted in the formation of D atoms. In fact there is some evidence to suggest that the loss mechanism for H_2CN on the walls at 200 K differs from that at 298 K. Measurement of the overall yield of HCN from the $N + CH_3$ reaction at 200 K gave a value of about 0.7, as opposed to a number much closer to 1 at 298 K. It is difficult to see how this measurement could give a value of anything other than 1 if only gas phase reactions are considered. It may be that the discrepancy is a result of an unusual wall-loss mechanism. In view of these problems, the D-atom experiments at 200 K are ignored.

Study at 363 K

The experiments described in the previous section to determine the yields of D_2 and D_2CN from the $N + CD_3$ reaction were repeated at 363 K. Virtually identical results were obtained and our results are summarized in Table IV. Although no calibration for H_2CN was performed, signal from the radical at $m/e = 28$ was readily detected supporting the assumption that these branching ratios are also applicable to the reaction of N atoms with the undeuterated methyl radical.

It was impossible to carry out experiments on the formation of D atoms, as at this temperature the wall loss of D atoms was sufficiently large to prevent even a calibration for D being obtained. F atoms were also found to be destroyed on the wall with a rate constant of about 30 s^{-1}. This heterogeneous loss process would complicate the analysis of results from the formation of HCN: consequently, no such experiments were performed.

Study at 423 K

Just as at the other temperatures the yield of D_2 from the $N + CD_3$ reaction in the presence of Cl_2 was found to be about 10%. Because of a huge wall loss for F atoms at this temperature ($k \sim 140\ s^{-1}$) it was impossible to measure accurate initial CD_3 concentrations in the region close to the

TABLE III. Branching ratios for reaction (1)[a] and (1D) at $T = 200$ K.

Channel	α(200 K)	Method
(1aD) $DCN + D_2$	0.11 ± 0.03	[D_2] vs. [CD_3] in presence Cl_2
(1bD) $DCN + 2D$	<0.4	Comparison between numerical simulation of D_2CN formation and calibration of D_2CN at 298 K
(1cD) $D_2CN + D$	$0.89^{+0.03}_{-0.39}$	Same as for (1bD)

[a]By analogy with study at 298 K, these branching ratios are adopted for reaction (1) also. This assumption is supported by the fact that H_2CN is easily detected at this temperature.

TABLE IV. Branching ratios for the reactions (1)[a] and (1D) at $T = 363$ K.

Channel	α(363 K)	Method
(1aD) $DCN + D_2$	0.12 ± 0.04	[D_2] vs. [CD_3] in presence of Cl_2
(1bD) $DCN + 2D$	<0.5	Comparison between computer model and calibration of D_2CN at 298 K
(1cD) $D_2CN + D$	$0.88^{+0.02}_{-0.48}$	Same as for (1bD)

[a]By analogy with study at 298 K, these branching ratios are adopted for reaction (1) also. This assumption is supported by the fact that H_2CN was easily detected at this temperature.

TABLE V. Branching ratios for the reactions (1) and (1D) at $T = 423$ K[a].

Channel	α(423 K)	Method
(1aD) DCN + D_2	0.10 ± 0.03	[D_2] vs. [CD_3] in presence of Cl_2

[a] No further quantitative studies were carried out. However, both H_2CN and D_2CN were readily detected at this temperature.

detection system. As a result it was not possible to use the calibration for D_2CN obtained at room temperature to estimate the branching ratios of reaction (1D) at 423 K. Attempts to carry out other quantitative experiments were abandoned for the same reasons they were at 363 K. However, the radicals H_2CN and D_2CN were detected at this temperature and in the absence of further evidence, we assume that the branching ratios are the same at 423 K as at the other temperatures. Table V summarizes the results obtained at $T = 423$ K.

Structure of the H_2CN radical

Up until now it has been assumed that the signal detected at $m/e = 28$ is due to H_2CN (both H atoms bonded to the C atom) rather than cis- or trans-HCNH. One of the drawbacks of mass spectrometric detection is that the technique gives no structural information and so it is not possible to show directly which isomer is being detected. However, H_2CN seems the more likely of the three isomers to be generated in the N + CH_3 reaction. Consideration of the geometry of the reacting species suggests that H_2CN will be formed most readily; H_2CN can result from a simple substitution reaction, whereas the HCNH isomers can only be formed via an addition-rearrangement-elimination mechanism. Furthermore, *ab initio* calculations[17] have shown that H_2CN lies lower in energy than the other two isomers and so on thermodynamic grounds is the expected product.

In principle, some information about the structure of the radical can be obtained from the ionization potential (IP) of the species detected at $m/e = 28$. By following the appearance potential for the species generated in reaction (1) at $m/e = 28$, an IP of (9.6 ± 1.0) eV was determined. The same result was obtained when the N + CD_3 system was studied and the IP of the species at $m/e = 30$ was measured. Determinations of the IPs of HCN and NO were used to calibrate the spectrometer. Unfortunately the IPs of the various CH_2N isomers are not known. We attempted to get some information by comparing our measured IP with the values obtained by applying Hess' law to the reactions

$$CH_3N_3 + e \rightarrow CH_2N^+ + N_2 + H + 2e, \quad \Delta H_{12} = 10.5 \text{ eV}^{18}, \tag{12}$$

and

$$CH_2N + N_2 + H \rightarrow CH_3N_3, \quad \Delta H_{13}, \tag{13}$$

giving

$$CH_2N + e \rightarrow CH_2N^+ + 2e, \quad \Delta H_{14} = \Delta H_{12} + \Delta H_{13}. \tag{14}$$

Heats of formation of H[13], CH_3N_3,[19] and CH_2N[17] have been measured or calculated and the $HCNH^+$ ion has been shown to lie 3.1 eV[20] lower in energy than H_2CN^+. However, the identity of CH_2N^+ in reaction (12) is not known and we were unable to determine which isomer of CH_2N was present in our system. A cycle based on the known heat of formation of CH_3NH_2[21] and the reaction

$$CH_3NH_2 + e \rightarrow CH_2N^+ + H_2 + H + 2e, \quad \Delta H_{15} = 15.2 \text{ eV}^{22} \tag{15}$$

suffered from this difficulty also. If it is assumed that H_2CN^+ is generated in reactions (12) and (15) and that H_2CN is generated in reaction (R1) a consistent picture is arrived at. However, assuming that $HCNH^+$ and trans- (or cis-) HCNH are the respective products of those processes also provides a reasonable description of the energetics. Consequently our IP measurement does not allow the unambiguous identification of the CH_2N isomer generated in reaction (1). However, on the basis of the available thermodynamic and mechanistic information we expect that the isomer is H_2CN.

DISCUSSION

Our results show that that at room temperature the reaction of N atoms with CH_3 proceeds to give H_2CN + H as the main channel with a small fraction of the reaction giving HCN + H_2. No isotope effect is observed when CH_3 is replaced by CD_3 and based on quantitative studies of the deuterated radical and qualitative studies of the undeuterated radical, the branching ratios appear to be independent of temperature. A number of questions must be asked. First, what are the reasons for the observed branching ratios? How do these results compare with those obtained for related reactions? How do the observations fit in with our knowledge of the dependence of the overall reaction rate on temperature? Finally, how do the results affect processes in which the N + CH_3 reaction is believed to play an important role? These questions will now be addressed in turn.

The reactants, $N(^4S_u)$ and $CH_3(^2A_2'')$ can react adiabatically on either a triplet or a quintet surface. The products $HCN(^1\Sigma^+) + H_2(^1\Sigma_g^+)$ can only give rise to a singlet surface, while the products $HCN(^1\Sigma^+) + 2H(^2S_g)$ and $H_2CN(^2B_2) + H(^2S_g)$ can form either a triplet or a singlet surface. Considering only conservation of spin assumes that the reaction proceeds via a transition state with no symmetry elements. Extending the analysis to a transition state of C_s symmetry shows that the reaction can proceed adiabatically on a $^3A''$ surface to give either HCN + 2H or H_2CN + H, but that HCN + H_2 gives rise only to a $^1A'$ surface which does not correlate with reactants. Both spin and orbital symmetry arguments give the same result; HCN + H_2 can only be generated after a forbidden surface crossing and so is expected to be formed inefficiently, as observed.

The triplet–singlet crossing is forbidden by the (approximate) intercombination selection rule.[23] However, spin–orbit coupling may lend some allowedness to this formally forbidden transition. Calculations based on the Landau–Zener formula[24] can, in principle, provide a measure of

the extent of the curve crossing. However, even for diatomic systems this method is not exact[23] and for more complex interactions drastic approximations are required. What can be done is to determine whether such a mechanism is symmetry allowed. In the absence of any symmetry elements, spin–orbit coupling must give rise to a state of species A_1 and is always allowed. In C_s symmetry the triplet spin function resolves into $A' + 2A''$, so the $^3A''$ state gives rise to states of overall symmetry species $^{es}A'' + 2^{es}A'$, where the superscript *es* identifies the species as being derived from both spin and orbital parts. Surface crossing can occur because the $^3A''$ species acquires some A' character as a result of spin–orbit coupling.

The reason why channel (1c) is preferred to (1b) seems to be linked to the energetics of the reaction system. The products $H_2CN + H$ lie approximately 100 kJ mol^{-1} lower in energy than HCN + 2H, favoring the former. Also, channel (1b) is only slightly exothermic which is not consistent with large rate constant measured for the overall reaction.[6] Furthermore, a steric effect may be in operation. We might expect that a hydrogen atom is most easily expelled from CH_3 when the outgoing H atom, the carbon atom and the incoming N atom are in an approximately linear configuration. This arrangement can be achieved if the incoming N atom attacks the carbon atom between the other two hydrogen atoms. Expulsion of 2 H atoms is likely to be most probable when $N–CH_2$ is planar. However, attaining this configuration is made difficult by the presence of the third H atom, and so reaction to give HCN + 2H is unfavorable. One would expect that at higher temperatures channel (1b) would become more important. Unfortunately our results are not sufficiently sensitive to test this hypothesis. Experiments performed at higher temperatures and with greater discrimination between channels will be required to do so.

Our experiments have provided results which are qualitatively in agreement with those expected on the basis of the energetics and orbital symmetry properties of the reactants and products. However, this agreement cannot be taken as proof that these factors are controlling the distribution of products, as is illustrated by the $O + CH_3$ reaction. The reaction between O atoms and methyl radicals is one of the few reactions which is closely related to reaction (1) and which has been extensively studied.[25] The process can give rise to products analogous to those possible for $N + CH_3$:

$$O + CH_3 \rightarrow HCO + H_2, \quad \Delta H = -358 \text{ kJ mol}^{-1}, \tag{16a}$$

$$O + CH_3 \rightarrow HCO + 2H, \quad \Delta H = +78 \text{ kJ mol}^{-1} \tag{16b}$$

$$O + CH_3 \rightarrow H_2CO + H, \quad \Delta H = -287 \text{ kJ mol}^{-1}. \tag{16c}$$

Niki *et al.*[26] have estimated that more than 85% of reaction (16) proceeds to give $H_2CO + H$, a result which corresponds to our observations on $N + CH_3$. However, in the case of reaction (16) all of the products are spin allowed (and symmetry allowed assuming the reaction proceeds with C_s symmetry), and thermodynamically, channel (16a) is favored. The implication of these observations is that product formation is determined by the dynamics of the molecular collisions, one H atom being easier to remove than one H_2 molecule. Clearly such an effect may be at work in the $N + CH_3$ reaction also. We are unable to distinguish between this factor and the symmetry/energetics reasoning.

One of the reasons for carrying out this study was the hope that it might shed some light on the temperature dependence observed for the $N + CH_3$ reaction.[6] The Arrhenius plot for this reaction appears to be non-linear, with the apparent activation energy increasing with temperature. A possible explanation of this behavior is that the T dependence is a result of the presence of two reactive channels with different individual temperature dependences. This study shows the branching ratios to be temperature independent, although the experiments are not very sensitive to small changes in the branching ratios. The two channel model, therefore, can not explain the T dependence of reaction (1).

This study represents the first direct measurement of the branching ratios of the $N + CH_3$ reaction. The most important result is that the methylene amidogen radical is generated in the major channel of the reaction, confirming the suggestion of Safrany[4] which was based on results from active nitrogen/hydrocarbon experiments. Although first detected in the gas phase many years ago by optical absorption,[27] little is known about H_2CN. That the radical is formed so efficiently in reaction (1) must complicate models used to describe Titan's atmosphere,[1] NO_x formation,[3] and HCN formation in circumstellar clouds.[2] For example, although Yung *et al.* recognized that reaction (1) could generate H_2CN, in their model of Titan's atmosphere they assumed the reaction gave HCN + 2H. The model must now include steps for the formation and destruction of the H_2CN species.

ACKNOWLEDGMENTS

This work was supported by the NASA Planetary Atmospheres Program. Fred L. Nesbitt acknowledges support under NASA Grant No. NSG-5173 to The Catholic University of America. George Marston thanks the National Research Council/National Academy of Sciences for the award of a Research Associateship.

[1] Y. L. Yung, M. Allen, and J. P. Pinto, Astrophys. J. Suppl. Ser. **55**, 465 (1984).
[2] L. A. M. Nejad and T. J. Millar, Mon. Not. R. Astron. Soc. **230**, 79 (1988).
[3] P. Glarborg, J. A. Miller, and R. J. Kee, Combust. Flame **65**, 177 (1986).
[4] D. R. Safrany, Progr. React. Kinet. **6**, 129 (1971).
[5] L. J. Stief, G. Marston, D. F. Nava, W. A. Payne, and F. L. Nesbitt, Chem. Phys. Lett. **147**, 570 (1988).
[6] G. Marston, F. L. Nesbitt, D. F. Nava, W. A. Payne, and L. J. Stief, J. Phys. Chem. (in press).
[7] J. Brunning and L. J. Stief, J. Chem. Phys. **84**, 4371 (1986).
[8] F. L. Nesbitt, W. A. Payne, and L. J. Stief, J. Phys. Chem. **92**, 4030 (1988).
[9] J. V. Michael, D. F. Nava, W. A. Payne, J. H. Lee, and L. J. Stief, J. Phys.

Chem. **83**, 2818 (1979), and references therein.
[10]M. A. A. Clyne and B. A. Thrush, Trans. Faraday Soc. **57**, 2176 (1961).
[11]F. L. Nesbitt, G. Marston, and L. J. Stief (in preparation).
[12]P. P. Bemand and M. A. A. Clyne, J. Chem. Soc. Faraday Trans. 2, **73**, 394 (1977).
[13]W. B. DeMore, *et al.*, *Chemical Kinetics and Photochemical Data for use in Stratospheric Modelling*, Evaluation No. 8, J. P. L. Publication 87-41 (1987).
[14]R. G. Manning, E. R. Grout, J. C. Merrill, J. P. Norris, and J. W. Root, Int. J. Chem. Kinet. **7**, 39 (1975).
[15]J. S. Levine, in *The Photochemistry of Atmospheres* (Academic, Orlando, 1985).
[16]P. R. Bevington, in *Data Reduction and Error Analysis for the Physical Sciences*, (McGraw-Hill, New York, 1969).
[17]R. A. Bair and T. H. Dunning, J. Chem. Phys. **82**, 2280 (1985).
[18]J. L. Franklin, V. H. Dibeler, R. M. Reese, and M. Krauss, J. Am. Chem. Soc. **80**, 298 (1958).
[19]S. W. Benson, F. R. Cruickshank, D. M. Golden, G. R. Haugen, H. E. O'Neal, A. S. Rodgers, R. Shaw, and R. Walsh, Chem. Rev. **69**, 279 (1969).
[20]M. P. Conrad and H. F. Schaefer, Nature **274**, 456 (1978).
[21]J. B. Pedley, R. D. Naylor, and S. P. Kirby in *Thermodynamic Data of Organic Compounds* (Chapman and Hall, London, 1986).
[22]J. E. Collin and M. J. Franskin, Bull. Soc. R. Sci. Liege **35**, 267 (1966).
[23]G. Herzberg, in *Molecular Spectra and Molecular Structure III. Electronic Spectra and Electronic Structure of Polyatomic Molecules.* (Van Nostrand, Princeton, 1966).
[24]R. G. Gilbert and I. G. Ross, Aust. J. Chem. **24**, 1541 (1971).
[25]I. R. Slagle, F. J. Pruss, and D. Gutman, Int. J. Chem. Kinet. **6**, 111 (1974). N. Washia and K. D. Bayes, Int. J. Chem. Kinet. **8**, 777 (1976); N. Washida, J. Chem. Phys. **73**, 1665 (1980); I. C. Plumb and K. R. Ryan, Int. J. Chem. Kinet. **14**, 861 (1982).
[26]H. Niki, E. E. Daby, and B. Weisenstock, J. Chem. Phys. **48**, 5729 (1968).
[27]J. F. Ogilvie and D. G. Horne, J. Chem. Phys. **48**, 2248 (1968).